4332 *Chem. Mater.* **2009,** *21,* 4332–4338
DOI:10.1021/cm901864z

CHEMISTRY OF MATERIALS
Article

The Ternary Nitrides $GaFe_3N$ and $AlFe_3N$: Improved Synthesis and Magnetic Properties

Andreas Houben, Jens Burghaus, and Richard Dronskowski*

Institut für Anorganische Chemie, RWTH Aachen University, Landoltweg 1, 52056 Aachen, Germany

Received June 29, 2009. Revised Manuscript Received August 7, 2009

The recently published two-step ammonolysis was adapted to the first synthesis of $GaFe_3N$ as a pure phase and $AlFe_3N$ with a very high phase purity. Similar to archetypal γ'-Fe_4N (a = 3.7900(6) Å), the ternary nitride $GaFe_3N$ adopts a perovskite-like structure in space group $Pm\overline{3}m$ with a slightly enlarged lattice parameter of a = 3.7974(1) Å. The magnetic characterization clearly evidences that $GaFe_3N$ is an antiferromagnet. The systematic exchange of Ga by Fe in going from $GaFe_3N$ to γ'-Fe_4N results in a change from antiferromagnetic to ferromagnetic behavior. In contrast, the homologous ternary nitride $AlFe_3N$ shows a statistical Al/Fe substitution which results in space group $Fm\overline{3}m$. $AlFe_3N$ can be classified as a soft ferromagnetic nitride.

Introduction

Within the past 60 years, a large number of ternary iron nitrides with the general formula MFe_3N have been investigated with regard to synthesis and structural and magnetic properties. Structurally, these nitrides are closely related to the binary nitride γ'-Fe_4N, which has been studied intensively using both experimental[1−3] and theoretical[4,5] methods. γ'-Fe_4N adopts an antiperovskite-like crystal structure (Figure 1) with space group $Pm\overline{3}m$ and a lattice parameter of a = 3.7900(6) Å.[3]

This archetypal ferromagnetic binary nitride possesses a remarkable chemical inertness and exhibits fascinating magnetic properties that make γ'-Fe_4N a possible material for high-performance magnetic recording heads. In particular, the very large saturation magnetization M_S = 208 Am^2kg^{-1} (which is close to that of α-Fe with M_S = 218 Am^2kg^{-1}) and also the low coercive field of H_C = 5.8 Oe ≈ 460 A m^{-1} have attracted early attention.[2] It is still important to improve materials for magnetic data storage, next to developing better technologies based on new physical phenomena. This is surely an anticipated synthetic challenge[6] for solid-state chemistry. Consequently, it is well-known that the magnetic properties of γ'-Fe_4N can be influenced by substituting the iron atoms on Wyckoff positions 1*a* and/or 3*c*. The newly introduced atoms mainly control the crystal growth, thereby yielding magnetic particles with a pronounced anisotropic shape and a high coercive field that makes them suitable for high-density storage materials.[7−9] As already mentioned, MFe_3N-type nitrides were synthesized using a wide range of metals (for an overview see Table 1). The results of preceding contributions can be found in ref 10. Additionally, nitrides with the formula $M_xFe_{4-x}N$ are formed with M = Co,[8] Cu,[11,12] Zn,[13] Ru,[7] Ag,[14] Os,[7] and Ir[7] ($x \ll 1$) as well as with Sn ($0 \le x \le 1.2$),[12,15−17] Mn,[9] and Ni[1,18−20] ($0 \le x \le 4$). For Ga[12], Ge[12] ($x \le 1$) and Al[21], other nitridic side-phases of M or iron were observed. The iron nitride with Mg[21] has only been briefly mentioned. Also, daltonide phase MFe_3N were obtained for M = Rh,[22,23] Pd,[24] Pt,[1] In,[12,13] and Au.[14] Eventually, many of the aforementioned nitrides plus a couple of hypothetical nitrides, yet to be synthesized, were investigated by theorists in order

*Corresponding author. E-mail: drons@HAL9000.ac.rwth-aachen.de. Fax: (+49) 241-80-92642.

(1) Wiener, G. W.; Berger, J. A. *J. Met.* **1955**, *7*, 360.
(2) Chen, S. K.; Jin, S.; Tiefel, T. H.; Hsieh, Y. F.; Gyorgy, E. M.; Johnson, D. W.Jr. *J. Appl. Phys.* **1991**, *70*, 6247.
(3) Jacobs, H.; Rechenbach, D.; Zachwieja, U. *J. Alloys Compd.* **1995**, *227*, 10.
(4) Matar, S.; Mohn, P.; Demazeau, G.; Siberchicot, B. *J. Phys.* (*Paris*) **1988**, *49*, 1761.
(5) Kuhnen, C. A.; De Figueiredo, R. S.; Drago, V.; da Silva, E. Z. *J. Magn. Magn. Mater.* **1992**, *111*, 95.
(6) Albrecht, M.; Thiele, J.-U.; Moser, A. *Physik Journal* **2003**, *10*, 25.
(7) Andriamandroso, D.; Matar, S.; Demazeau, G.; Fournès, L. *IEEE Trans. Magn.* **1993**, *29*, 2.
(8) Matar, S.; Fournès, L.; ChéRubin-Jeannette, S.; Demazeau, G. *Eur. J. Solid State Inorg. Chem.* **1993**, *30*, 871.
(9) Siberchicot, B.; Matar, S. F.; Fournès, L.; Demazeau, G.; Hagenmüller, P. *J. Solid State Chem.* **1990**, *84*, 10.
(10) Stadelmaier, H. H. *Z. Metallkd.* **1961**, *52*, 758.
(11) de Figueiredo, R. S.; Foct, J.; dos Santos, A. V.; Kuhnen, C. A. *J. Alloys Compd.* **2001**, *315*, 42.
(12) Stadelmaier, H. H.; Fraker, A. C. *Z. Metallkd.* **1962**, *53*, 48.
(13) Kuhnen, C. A.; De Figueiredo, R. S.; dos Santos, A. V. *J. Magn. Magn. Mater.* **2000**, *219*, 58.
(14) Figueiredo, R. S.; Kuhnen, C. A.; dos Santos, A. V. *J. Magn. Magn. Mater.* **1997**, *173*, 141.
(15) Andriamandroso, D.; Fefilatiev, L.; Demazeau, G.; Fournès, L.; Pouchard, M. *Mater. Res. Bull.* **1984**, *19*, 1187.
(16) Zhao, Z. J.; Xue, D. S.; Li, F. S. *J. Magn. Magn. Mater.* **2001**, *232*, 155.
(17) Zhao, Z.; Xue, D.; Chen, Z.; Li, F. *Phys. Status Solidi A* **1999**, *174*, 249.
(18) Li, F.; Yang, J.; Xue, D.; Zhou, R. *Appl. Phys. Lett.* **1995**, *66*, 2343.
(19) Rochegude, P.; Foct, J. *Ann. Chim.* **1983**, *8*, 533.
(20) Shirane, G.; Takei, W. J.; Ruby, S. L. *Phys. Rev.* **1962**, *126*, 49.
(21) Stadelmaier, H. H.; Yun, T. S. *Z. Metallkd.* **1961**, *52*, 477.
(22) Houben, A.; Müller, P.; von Appen, J.; Lueken, H.; Niewa, R.; Dronskowski, R. *Angew. Chem., Int. Ed.* **2005**, *44*, 7212. *Angew. Chem.* **2005,** *117*, 7379.
(23) Houben, A.; Šepelák, V.; Becker, K.-D.; Dronskowski, R. *Chem. Mater.* **2009**, *21*, 784.
(24) Stadelmaier, H. H.; Fraker, A. C. *Trans. Metallurg. Soc. Aime* **1960**, *218*, 571.

Published on Web 08/26/2009

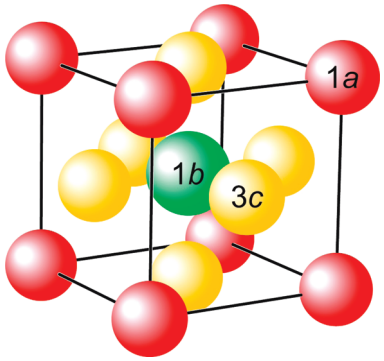

Figure 1. Crystal structure of γ'-Fe_4N in space group $Pm\bar{3}m$ (a = 3.7900(6) Å).[3] The nitrogen atom (green) occupies the very center (Wyckoff position 1*b*), and the iron atoms (red/yellow) are found at the corners (1*a*) and face centers (3*c*). In $GaFe_3N$ the iron atoms at the 1*a* corner positions are almost fully replaced by gallium atoms. Because $AlFe_3N$ adopts space group $Fm\bar{3}m$, the iron and aluminum atoms statistically occupy the corner and face-centered positions (4*a*) with a 3:1 ratio while every fourth body-centered site (25%) is occupied by nitrogen (4*b*).

to characterize their structural, magnetic, and mechanical properties.[14,25−43]

The substitutional preference of the M atom to go on Wyckoff position 1*a* and/or 3*c* depends on the relative affinities of Fe or M to the nitrogen atom and, even more important, on the relative sizes of the metallic radii.[44] Only if the metallic radius of the substituting M atom is larger than that of the Fe atom is position 1*a* clearly preferred, simply because the coordination sphere of the 1*a*-centered cuboctahedron (see Figure 1) is much larger than the one of the 3*c* position.[22]

After studying the iron−gallium−nitrogen phase diagram, the first synthesis of $GaFe_3N$[12] was already published by Stadelmaier and Fraker in 1962. A total of five compositions with different Ga:Fe atomic ratios between 0.3:3 up to 1.3:3 were synthesized using classical NH_3/H_2 ammonolysis reactions at 600 °C. The reactants were powdered alloys, and the target compositions were established by previous sintering reactions. Although no diffractogram had been given, all phases were stated to exhibit the crystallographic symmetry of γ'-Fe_4N, namely $Pm\bar{3}\,m$. Independent of the amount of incorporated Ga, all phases exhibit a lattice parameter of a = 3.80 Å, which is close to that of γ'-Fe_4N despite the fact that the metallic radius of gallium r_M(Ga) = 1.41 Å[45] is much larger than that of iron. This is difficult to understand in the context of an anticipated Vegard-like relationship between lattice parameters and chemical compositions but probably hidden under the unknown error bars of the published lattice parameters. According to the authors, gallium seems to have a wide solubility range in the binary iron nitride. Nevertheless, each synthesis is accompanied by the hexagonal side-phase GaN.[46] Unfortunately, the lattice parameters and the GaN weight fractions were not reported. Furthermore, a theoretical investigation of the ternary nitride $GaFe_3N$ is still missing.

Another contribution of Stadelmaier and Yun describes the aluminum−iron−nitrogen system.[21] By using an analogous synthesis the authors arrived at "$Al_{43}Fe_{43}N_{14}$" next to the side-phase AlN. The ternary nitride is characterized by a lattice parameter of a = 3.80 Å and possesses the γ'-Fe_4N-analogous structure. Thus, also the solubility range of Al in γ'-Fe_4N seems to be relatively large. Other Fe:Al ratios resulted in different structures, e.g., the ε-Fe_3N-related ternary nitride.

It is difficult to avoid a side-phase during the synthesis of such ternary iron nitrides because these often have a low free energy of formation. An example on how to improve the phase purity is given by the itinerant ferromagnet and ternary nitride $RhFe_3N$ that was investigated by our group.[22,23,25] The recently published two-step ammonolysis method combines a high-temperature (1000−1300 °C) sintering step and a low-temperature (ca. 500−600 °C) nitriding reaction (see Figure 2) to give $RhFe_3N$ with a significantly improved phase purity.[23] The lower temperature may be looked upon as fairly typical for the nitridation of γ'-Fe_4N and related ternary nitrides. A temperature ramp is introduced between the two reactions to yield the slightly more stable nitride under thermodynamically controlled conditions.

Results and Discussion

A phase-pure synthesis of $GaFe_3N$ was achieved by varying the synthesis parameters, that is, the sintering temperature and the duration of the two-step ammonolysis synthesis. The phase-pure nitride was made with a high-temperature (1100 °C) and a brief sintering reaction ahead of the actual nitridation reaction. As already described by Stadelmaier, we observed the side phase GaN for sintering temperatures lower than 1100 °C. The diffractogram (see Figure 3) clearly evidences that $GaFe_3N$ possesses an, at least partially, ordered structure, i.e., the typical perovskite-like γ'-Fe_4N-analogous structure in space group $Pm\bar{3}m$

(25) von Appen, J.; Dronskowski, R. *Angew. Chem., Int. Ed.* **2005**, *44*, 1205. *Angew. Chem.* **2005**, *117*, 2.
(26) Music, D.; Schneider, J. M. *Appl. Phys. Lett.* **2006**, *88*, 031914.
(27) Dronskowski, R. *Computational Chemistry of Solid State Materials*; Wiley-VCH: Weinheim, Germany, 2005.
(28) dos Santos, A. V.; Kuhnen, C. A. *J. Alloys Compd.* **2001**, *321*, 60.
(29) Kuhnen, C. A.; dos Santos, A. V. *Solid State Commun.* **1993**, *85*, 273.
(30) dos Santos, A. V.; Krause, J. C.; Kuhnen, C. A. *Physica B* **2006**, *382*, 290.
(31) Kuhnen, C. A.; dos Santos, A. V. *J. Alloys Compd.* **2004**, *384*, 80.
(32) Kuhnen, C. A.; de Figueiredo, R. S.; dos Santos, A. V. *J. Magn. Magn. Mater.* **2000**, *219*, 58.
(33) Paduani, C. *J. Magn. Magn. Mater.* **2004**, *278*, 231.
(34) Chen, L. *J. Appl. Phys.* **2006**, *100*, 113717.
(35) Paduani, C. *J. Appl. Phys.* **2003**, *96*, 1503.
(36) Kuhnen, C. A.; dos Santos, A. V. *J. Alloys Compd.* **2000**, *197*, 68.
(37) Kuhnen, C. A.; dos Santos, A. V. *J. Magn. Magn. Mater.* **1994**, *130*, 353.
(38) Mohn, P.; Schwarz, K.; Matar, S.; Demazeau, G. *Phys. Rev. B* **1992**, *45*, 4000.
(39) dos Santos, A. V.; Krause, J. C. *J. Magn. Magn. Mater.* **2004**, *283*, 297.
(40) Krause, J. C.; Paduani, C. *Physica B* **2005**, *367*, 282.
(41) Matar, S.; Mohn, P.; Kübler, J. *J. Magn. Magn. Mater.* **1992**, *104*, 1927.
(42) Wu, Z.; Meng, J. *Appl. Phys. Lett.* **2007**, *90*, 241901.
(43) Zhao, E.; Xiang, H.; Meng, J.; Wu, Z. *Chem. Phys. Lett.* **2007**, *449*, 96.
(44) Cordier-Robert, C.; Foct, J. *Eur. J. Solid State Inorg. Chem.* **1992**, *29*, 39.
(45) Pauling, L. *J. Am. Chem. Soc.* **1947**, *69*, 542.
(46) Juza, R.; Hahn, H. *Z. Anorg. Allg. Chem.* **1938**, *239*, 282.

Table 1. Overview of Current Synthetic and Theoretical Contributions Targeted at MFe_3N Type Nitrides As Published in the Literature[a]

										Al*	
Ti	V	Cr	Mn	Fe	Co	Ni	Cu	Zn	Ga*	Ge*
				Ru	Rh*	Pd	Ag		In	Sn
				Os	Ir	Pt	Au			

M	theoretical investigations available
M*	main phase is accompanied by one or more side-phases
M	small amount/occupation of the substituting metal
M	wide range of occupations possible; also larger than 1.0
M	phases with an occupation of M that is close to 1.0

[a] An underlined element symbol indicates a theoretical investigation. An asterisk shows that the synthesis is accompanied by one or more side-products. Furthermore, the background color is an indicator of the occupation with regard to the substituting metal M.

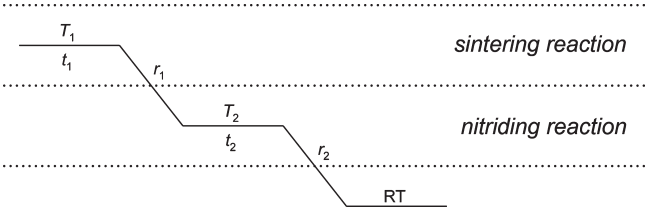

Figure 2. Schematic diagram showing the two-step ammonolysis reaction with a high-temperature (1000−1300 °C) sintering step and a low-temperature (ca. 500−600 °C) nitriding reaction. Between the two reactions, a temperature ramp is introduced to yield the slightly more stable nitride under thermodynamically controlled conditions.

including the low-angle reflections (100) and (110), which are not observed in the disordered structure with space group $Fm\bar{3}m$. The lattice parameter of $a = 3.7974(1)$ Å is in excellent agreement with the literature.

In analogy to the investigations on the ternary nitride $RhFe_3N$[22,23] the occupation of position 1*a* with either gallium and/or iron deserves a closer attention. In the Rietveld refinements, the 1*a* occupation parameter was therefore split into two, and the iron and gallium site occupations were constrained to unity. The refined Ga occupation arrived at 90(10)%. Assuming that gallium, because of its larger metallic radius, exclusively occupies position 1*a* but not position 3*c*, the gallium occupation for position 1*a* can also be calculated on the basis of the iron/gallium ratio (k_a = at %(Fe)/at %(Ga)) measured by atom absorption spectroscopy (AAS). Because of the space group $Pm\bar{3}m$, the iron and gallium site multiplicity of positions 1*a* and 3*c* always sum up to ${}^{1a}x^{Ga}_{Occ} + x(Fe) = 4$ with $x(Fe) = {}^{1a}x^{Ga}_{Occ}k_a$ using the aforementioned assumption. Combining both formulas and solving for the gallium occupation on position 1*a* one arrives at ${}^{1a}x^{Ga}_{Occ} = 4/(1 + k_a) = 75(10)\%$. With respect to the limited gallium sensitivity of the AAS method, this occupation is in good agreement with the refined XRD value. Additional measurements using SEM/EDX spectroscopy again resulted in a gallium occupation of around 90(10)% (see Figure 4). Thus, the correct formula must be $Ga_{0.9}Fe_{3.1}N$. For the sake of simplicity, we will continue to use the formula $GaFe_3N$.

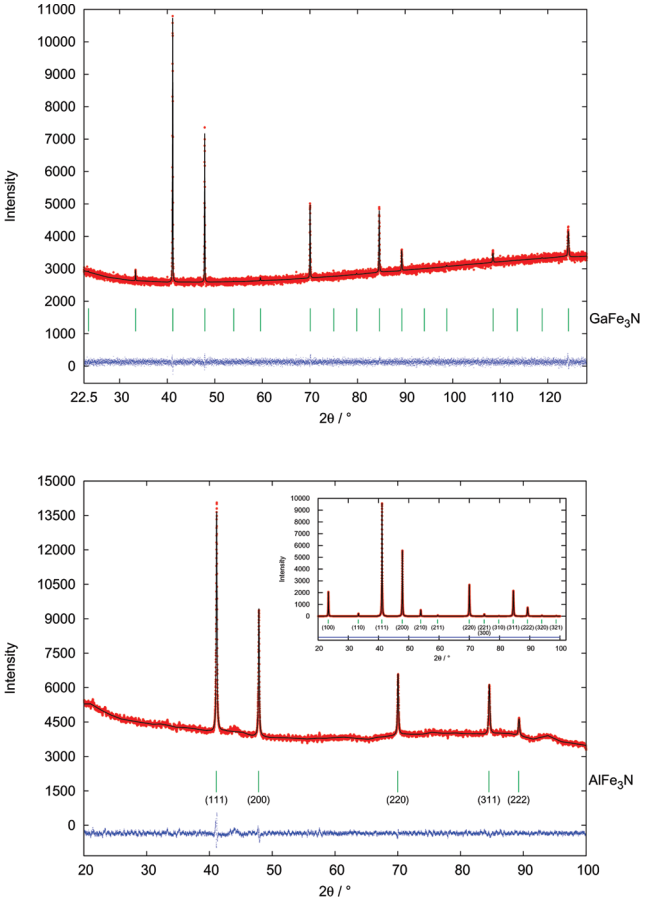

Figure 3. X-ray diffraction pattern and Rietveld refinement plot of $GaFe_3N$ ($Pm\bar{3}m$; $a = 3.7974(1)$ Å, above) and $AlFe_3N$ ($Fm\bar{3}m$; $a = 3.7967(3)$ Å, below). The vertical bars designate the positions of the Bragg reflections and the corresponding (*hkl*) indices. The inset in the $AlFe_3N$ plot shows the simulated pattern of $AlFe_3N$ using the erroneous space group $Pm\bar{3}m$ (Al on 1*a*, Fe on 3*c*, N on 1*b*) and the profile parameters of the correctly refined pattern.

The magnetic properties of $GaFe_3N$ were determined by SQUID magnetometry (MPMS-5S, Quantum Design) in the temperature range of 100−400 K at applied fields of $B_0 = 0.03$ T and $B_0 = 0.1$ T. Although the Néel temperature cannot be clearly determined, the paramagnetic Curie−Weiss temperature is slightly negative (θ_p between −22 and −10 K),

indicating a weak antiferromagnetic coupling (see Figure 5, left). A hysteresis loop was recorded at a temperature of 5 K within a field range of ± 5 T (see Figure 5, right). Up to the applied field of $B_0 = 5$ T, the magnetization of the sample is not saturated, and the unsaturated magnetic moment, possibly because of the minor Fe occupation of the 1*a* site in $GaFe_3N$, reaches a value of $\mu_a^s = 0.87(1)\,\mu_B$ per formula unit. In accordance with the antiferromagnetic behavior, the coercive field H_C and the remanent magnetization are negligible. Thus, the hysteresis measurement of $GaFe_3N$ is indicative of an antiferromagnetic material, too. Because the other known ternary iron nitride of main group III, namely $AlFe_3N$ (see below), is characterized as a ferromagnetic and $InFe_3N$ as a paramagnetic material,[32] the role of Ga with respect to the decay of the ferromagnetic behavior is noteworthy. Neutron diffraction studies are planned to determine the spin ordering.

Finally, temperature-dependent X-ray diffraction experiments were carried out up to 630 °C to determine the decomposition temperature of $GaFe_3N$. As can be seen from Figure 6 (top), the decomposition starts at about 540 °C and is completed above 600 °C; the $GaFe_3N$ reflections disappear in between. This finding is analogous to the previously synthesized ternary nitride $RhFe_3N$, which revealed a decomposition temperature of 530 °C.[22]

To get a better understanding of the evolution of the lattice parameters and the magnetic properties between

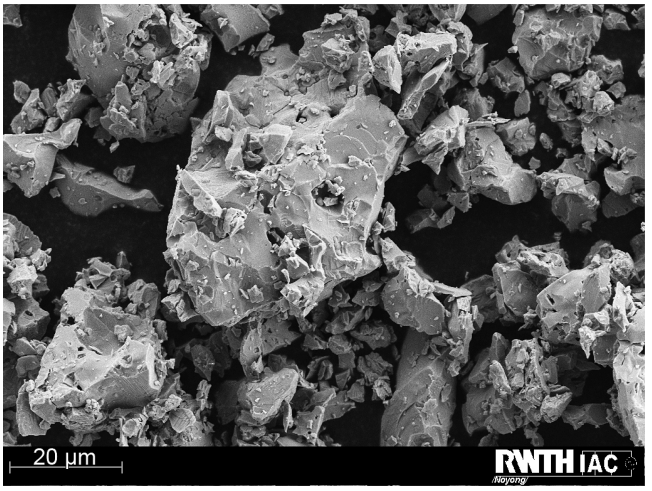

Figure 4. Particle size distribution for $GaFe_3N$ determined by scanning electron microscopy; EDX spectroscopic measurements were repeated for different spots to give an average gallium occupation on position 1*a* of 90(10)% (see text).

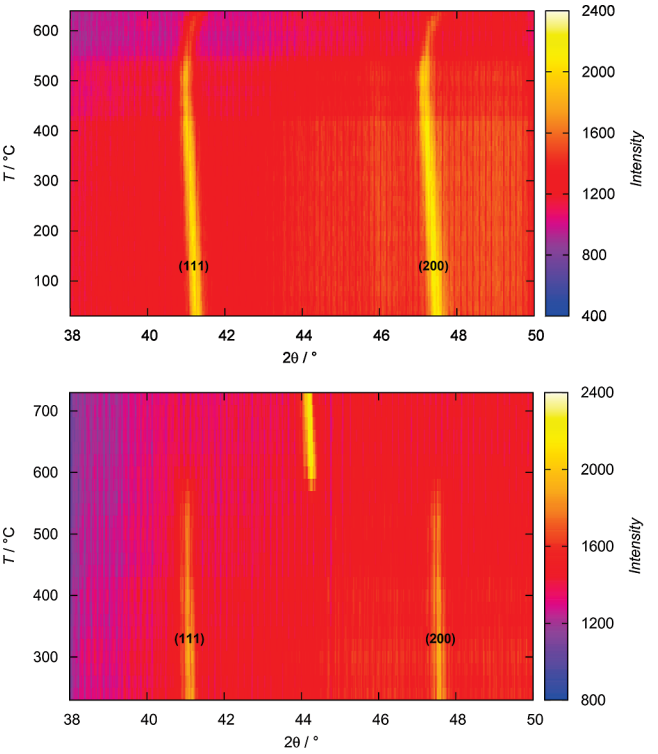

Figure 6. Temperature-dependent X-ray diffraction of $GaFe_3N$ (top) and $AlFe_3N$ (bottom) in the 2θ range between 38 and 50°; the two individual reflections with the highest intensity have been indicated. Both nitrides are stable up to a temperature of approximately 540 °C and decompose at higher temperatures. In the case of $AlFe_3N$, the formation of an iron−aluminum alloy can be observed by the new reflection at 44°.

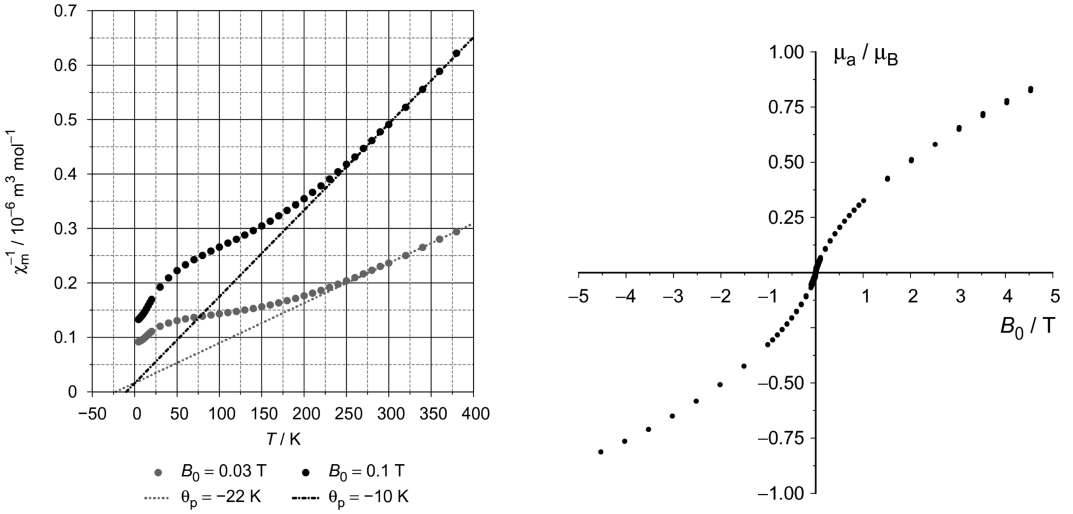

Figure 5. Reciprocal molar magnetic susceptibility for $GaFe_3N$ at applied fields of $B_0 = 0.03$ T and $B_0 = 0.1$ T as a function of temperature (left) and the hysteresis loop of $GaFe_3N$ at 5 K (right).

Table 2. Ideal Composition x of the $Ga_xFe_{4-x}N$ series, together with lattice parameter a, occupation of Ga on the 1a position $^{1a}x_{Occ}^{Ga}$, Gaussian−Lorentzian η mixing parameters and related Bragg values, molar mass M and X-ray density ρ

x	a (Å)	$^{1a}x_{Occ}^{Ga}$	η	R_p (%)	R_B (%)	M (g mol^{-1})	ρ (g cm^{-3})
0.90	3.7974(1)	0.9(1)	0.42	1.43	3.77	251.27	7.62
0.75	3.7974(1)	0.8(1)	0.48	1.55	8.68	247.80	7.51
0.625	3.7958(1)	0.6(1)	0.61	1.01	1.29	246.07	7.47
0.50	3.7941(1)	0.5(1)	0.42	1.35	2.96	244.33	7.43
0.375	3.7934(1)	0.4(1)	0.66	1.30	5.39	242.60	7.38
0.25	3.7929(1)	0.2(2)	0.51	1.44	6.32	240.86	7.33

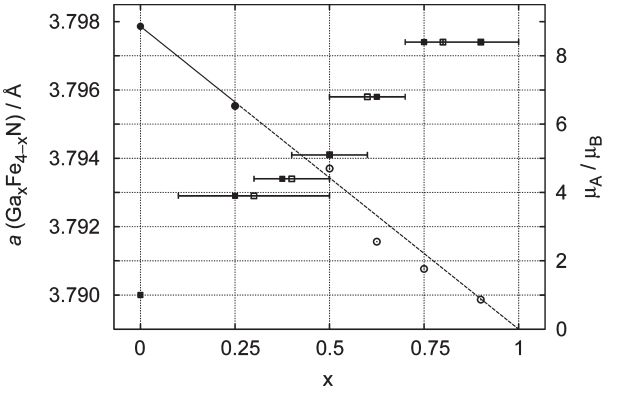

Figure 7. Change of the lattice parameter a (left) based on the intended (■) and the refined composition (□) as well as the atomic saturation moments (right) μ_A (●) and the unsaturated moments (○) for the entire $Ga_xFe_{4-x}N$ series of compounds. Note that the phase simplified as $GaFe_3N$ has a composition of $Ga_{0.9}Fe_{3.1}N$ (see text). The error bars indicate the uncertainty of the occupation on position 1a. With respect to the lattice parameters, their error bars are smaller than the data points themselves.

the limiting case of the archetype γ'-Fe_4N and the compound $GaFe_3N$, several compounds within the Ga_x-$Fe_{4-x}N$ series with $x = 0.25$, 0.50, 0.625, and 0.75 were synthesized and characterized. Compositional and structural parameters are listed in Table 2.

With respect to the refined occupation of position 1a, the occupation is prone to systematic error because the Ga and Fe X-ray atomic form factors are quite close to each other. Nevertheless, the compositions of all synthesized compounds are in good agreement with the ideal compositions.

Figure 7 (left ordinate) shows the refined lattice parameters as a function of the composition. γ'-Fe_4N exhibits a lattice parameter of $a = 3.7900(6)$ Å. The substitution of one-quarter of the Fe atoms on Wyckoff position 1a leads to the composition $Ga_{0.25}Fe_{3.75}N$ and a slightly larger lattice parameter of $a = 3.7929(1)$ Å, a likely consequence of the larger metallic radius of Ga (r_{Ga} = 1.41 Å)[45] compared to Fe (r_{Fe} = 1.24 Å).[45] The further incorporation of Ga, realized in $Ga_xFe_{4-x}N$ with x = 0.375, 0.5, 0.625, 0.75 increases the lattice parameter up to $a = 3.7974(1)$ Å. The (almost) full occupation of the 1a site finally results in the formation of the $GaFe_3N$, which exhibits the same lattice parameter as $Ga_{0.75}Fe_{3.25}N$ such that a Vegard-type trend is obvious.

The magnetic characterization of the $Ga_xFe_{4-x}N$ series reveals an almost linear decrease for the magnetic moments in going from γ'-Fe_4N (μ_a^s(5 T) = 8.86 μ_B) via

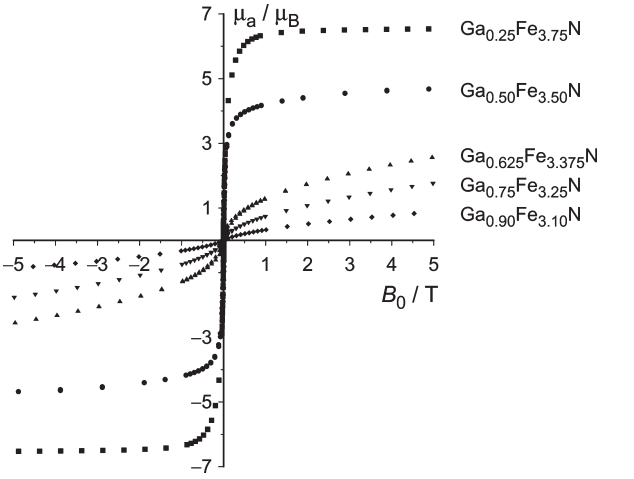

Figure 8. Hysteresis loops of $Ga_{0.25}Fe_{3.75}N$ (■), $Ga_{0.50}Fe_{3.50}N$ (●), $Ga_{0.625}Fe_{3.375}N$ (▲), $Ga_{0.75}Fe_{3.25}N$ (▼), and $Ga_{0.90}Fe_{3.10}N$ (♦) at 5 K. Magnetic saturation, the remanent magnetization as well as the coercive field lower with an increasing gallium concentration.

$Ga_{0.25}Fe_{3.75}N$ down to $GaFe_3N$ (μ_a(5 T) = 0.87 μ_B), illustrated by the likewise Vegard-type line in Figure 7 (right ordinate). It is important to recall that only the sample with $x = 0.25$ is saturated with respect to the magnetic moment whereas the samples with $x \geq 0.5$ (open symbols) are unsaturated at 5 T and 4 K. Thus, for $x \geq 0.5$, the saturated magnetic moments may be expected to be even larger (see Figure 8). The incorporation of Fe into the crystal structure increases the total magnetic moment by the substitution of the magnetically inactive Ga element. We suggest a change from the ferromagnetic $Ga_{0.5}Fe_{3.5}N$ to the antiferromagnetic $GaFe_3N$. Such a complete occupation of the 1a position by Ga results in a decay of the ferromagnetic ordering.

A systematic theoretical investigation is currently under preparation.

The homologous ternary nitride $AlFe_3N$ is insufficiently described in the literature. Other aluminum−iron nitrides were synthesized together with other side phases (see above).[21] By optimizing the parameters of the two-step ammonolysis, the nitride $AlFe_3N$ was synthesized in almost phase-pure form, with the exception of a very small and broad reflection at about $2\theta = 44°$ that has not yet been attributed to another known phase. In contrast to most MFe_3N nitrides, $AlFe_3N$ is not an ordered structure with space group $Pm\bar{3}m$ but can be described with a statistical occupation of iron and aluminum (ratio 3:1) in space group $Fm\bar{3}m$. Here, the metals form the face-centered cubic packing (position 4a), whereas the nitrogen statistically occupies one-fourth (25%) of the octahedral sites (position 4b). This result is immediately obvious from a comparison between both structures and space groups on the basis of structure-factor calculations, as seen from the corresponding diffraction patterns (see Figure 3, bottom). The refinement of the constrained occupation parameters of both metals (position 4a) evidences correct composition.

Temperature-dependent X-ray diffraction experiments were carried out up to 730 °C to determine the decomposition

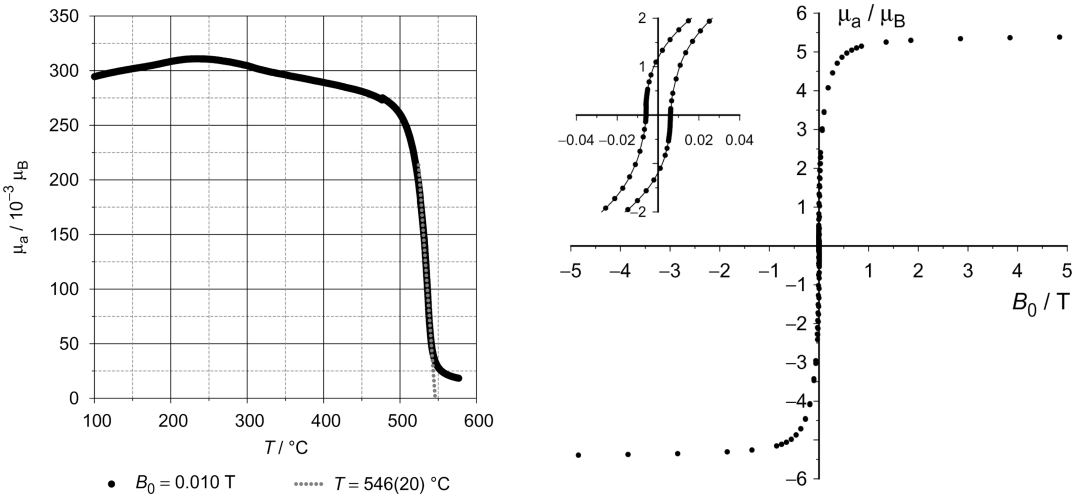

Figure 9. Variation of the magnetic moment μ_a per formula unit $AlFe_3N$ at a field of $B_0 = 0.01$ T as a function of temperature (left) and the hysteresis loop of the ferromagnetic $AlFe_3N$ at 5 K (right); in the latter, a part of this loop (insert) displays the remanent magnetization and the coercive field. The solid lines in the insert only serve to guide the eye.

temperature of $AlFe_3N$. As it can be seen from Figure 6 (bottom), the decomposition starts at about 540 °C and is completed above 600 °C. Within this temperature range the $AlFe_3N$ reflections disappear, and the formation of a new reflection of an iron−aluminum−alloy can be observed. This finding is again similar to the previously discussed nitride $GaFe_3N$ and to the ternary nitride $RhFe_3N$ with a decomposition temperature of 530 °C.[23]

Additionally, the measurement of the magnetic moment using a vibrating sample magnetometer (PPMS/VSM) at an applied field of $B_0 = 0.01$ T as a function of the temperature shows a strong temperature dependency in the range from 500−600 °C (see Figure 9). Upon extrapolating the linear fit of the steepest part of the magnetization curve to the intersection with the temperature axis, one finds a temperature of $T = 546(20)$ °C for $AlFe_3N$. Because this temperature is in excellent agreement with the decomposition temperature determined above, it is obvious that the sample decomposed during the measurement. The finding was fully reproduced using a new sample. Thus, the Curie temperature is not reached before the decomposition process begins, such that T_C of $AlFe_3N$ is much higher than that of $RhFe_3N$ (T_C = 505(25) K).[22] A further magnetic characterization using a SQUID magnetometer clearly shows that $AlFe_3N$ is ferromagnetic like the archetype γ'-Fe_4N. Within the hysteresis loop the specific saturation magnetization measured at 5 T reaches a value of $\sigma_s = 144(2)$ A m^2 kg^{-1} (see Figure 9). In comparison to γ'-Fe_4N, this is about 30% smaller, simply because of the missing magnetic moment of one Fe atom. Next to that, the coercive field is 10 times smaller than the one of γ'-Fe_4N. These findings and the remanence of $\mu_0 M_R = 0.25(2)$ T allow us to classify $AlFe_3N$ as a soft magnetic material.

Conclusion

In summary, the two-step ammonolysis yielded the first phase-pure synthesis of the ternary nitride $GaFe_3N$ and the homologous nitride $AlFe_3N$ with very high phase purity. $GaFe_3N$ adopts a perovskite-like structure ($Pm\bar{3}m$) with a lattice parameter of $a = 3.7974(1)$ Å in which Ga exclusively occupies the 1*a* position. AAS and EDX measurements suggest a slightly reduced gallium occupation resulting in the formula $^{1a}(Ga_{0.9}Fe_{0.1})^{3c}$-$Fe_3{}^{1b}N$. The magnetic properties evidence an antiferromagnetic behavior. In the series $Ga_xFe_{4-x}N$ the magnetic moment increases with an increasing amount of iron on position 1*a*. Thus, a systematic change from a ferromagnetic to an antiferromagnetic ordering takes place. Theoretical studies and further experiments, e.g., neutron diffraction studies, are necessary to understand the role of Ga with respect to the decay of the ferromagnetic ordering and to determine the spin ordering and the magnetic properties. For the first time the phase $AlFe_3N$ is characterized as a soft itinerant ferromagnet with a lattice parameter of $a = 3.7967(3)$ Å, which can be described, different from $GaFe_3N$, with a statistical occupation of iron and aluminum (ratio 3:1) on position 4*a* in space group $Fm\bar{3}m$.

Experimental Section

Synthesis of $GaFe_3N$ ($AlFe_3N$). The powdered reactants Ga_2O_3 (Al) and Fe_2O_3 were mixed and accurately ground using a stoichiometric ratio of 1:3 for the metal atoms. For the optimized synthesis the following parameters (see Figure 2) were used: $T_1 = 1100$ °C ($T_1 = 1100$−1200 °C), $t_1 = 1$ min, $T_2 = 500$ °C, $t_2 = 3$ h. The ammonolysis gas was a NH_3:H_2 mixture with a 1:1 ratio.

XRD and Rietveld Refinement. X-ray diffraction at room temperature for $Ga_xFe_{4-x}N$ was performed using a calibrated STADI MP (STOE Darmstadt) powder diffractometer with Cu Kα_1 radiation ($\lambda = 1.54059$ Å; flat sample; $5 \le 2\theta \le 130°$, step rate 0.01° in 2θ). The same procedure was carried out for $AlFe_3N$ on a Huber G670 Image plate powder diffractometer with Cu Kα_1 radiation ($\lambda = 1.54059$ Å; flat sample; $5 \le 2\theta \le 100°$, step rate 0.005° in 2θ). The Rietveld refinement was carried out with the program FullProf[47] and a pseudo-Voigt profile

(47) Rodriguez-Carvajal, J. *FULLPROF version 4.0*; Institut Laue-Langevin: Grenoble, France, 2007.

function. The refinement parameters and the residual values for the series of $Ga_xFe_{4-x}N$ are listed in Table 2. The positions are 1*a* for Ga, 1*b* for N, and 3*c*/1*a* for Fe within space group $Pm\bar{3}m$. By constraining the sum of the occupation parameters of iron and the main-group III metal on 1*a* to unity, the metal contribution for this position can be refined. Likewise, the iron occupation on position 3*c* was refined to be 100%.

For $AlFe_3N$, the formula weight is $M = 208.53$ g/mol with a cell volume of $V = 54.730(3)$ Å^3. The X-ray density is $\rho = 6.33$ g cm^{-3}. The refined lattice parameter of $AlFe_3N$ is $a = 3.7967(3)$ Å. The constrained occupation refinement results in the correct composition of $Al_{1.0(1)}Fe_{3.0(1)}N$. Thus, the Wyckoff positions within space group $Fm\bar{3}m$ are 4*a* for Fe/Al (fully occupied) and 4*b* occupied by 25% with N.

SEM/EDX. We used a LEO Supra 35 VP (LEO electron microscopy, Cambridge) for the SEM and an INCA Energy 200 (Si(Li)-crystal) from Oxford Instruments for the EDX analysis.

SQUID. The magnetic properties of all samples, except the temperature-dependent measurement of the magnetic moment for the $AlFe_3N$ sample, were determined by SQUID magnetometry (MPMS-5S, Quantum Design) in the temperature range 2−360 K and at applied fields between $B_0 = 0.005$ and 0.02 T. Hysteresis loops were recorded at a temperature of 5 K in the field range ±5 T.

PPMS/VSM. The temperature-dependent measurement of the magnetic moment of the $AlFe_3N$ sample was carried out using a Vibrating Sample Magnetometer (PPMS, Quantum Design with VSM/Oven options) in the temperature range 350−850 K and at an applied field of $B_0 = 0.01$ T.

Acknowledgment. It is a pleasure to thank Dr. Paul Müller for having performed the temperature-dependent X-ray measurements, Dr. Michael Noyong and Kerstin Blech for the SEM/EDX analysis, Dr. M. Speldrich, Prof. Dr. H. Lueken for the SQUID measurements, Anne Möchel, Berthold Schmitz for assistance during the PPMS measurements, and Deutsche Forschungsgemeinschaft for having funded this study.